

Study on the aerodynamic performance of the racing car rear spoiler by CFD technology

Leishuo Yang¹

¹Kang chiao international school (east China), No.500, Xihuan Rd., Huaqiao
Economic Development Zone, Kuanshan City, Jiangsu, China

727297yang@gmail.com

Abstract. The rear spoiler is one of the main components that affect the aerodynamic performance of the F1 racing car. At present, numerical simulation technology is becoming a research hotspot to study the aerodynamic performance of the F1 racing car. In this paper, we discuss the F1 racing car rear spoiler airfoil selection and three-dimensional design and use three-dimensional simulation software to calculate the impact of different attack angles, velocity, and airfoils on the rear spoiler's drag force and negative lift. The results show that the RAE2822 airfoil has a good lift-drag ratio at low velocity. When the attack angle is 30°, the maximum lift-drag ratio can be obtained. When the velocity exceeds 60 m/s, the impact on the lift-drag ratio is almost negligible.

Keywords: racing car rear spoiler, aerodynamics, numerical simulation, aerodynamic performance

1. Introduction

As the highest level of motor racing in the world today, the FIA Formula 1 World Championship has attracted the attention of fans all over the world. The Formula 1 car is a product of ingenuity and high technology, and complex aerodynamic design is essential to maximize the performance of the car, among other factors (e.g., engine, tyres). First of all, velocity is the key to winning a car race. Good aerodynamic modeling can make the car generate small aerodynamic resistance in high-velocity driving, thus greatly improving the power of the car. Secondly, because the car velocity is quite high, modern Formula 1 cars, for example, typically generate about 750 kilograms (or 1,653 pounds) of negative lift at the velocity of 100 MPH, a strong negative lift that gives the driver better control over high velocity. Therefore, good aerodynamic modeling is needed to make it generate huge negative lift at high velocity and ensure its operating stability. Among the aerodynamic components of a racing car, the rear spoiler, also known as the rear wing, is a key component that affects the aerodynamic characteristics of the car. The rear spoiler has a great influence on the aerodynamic characteristics of the car, such as changing the aerodynamic drag coefficient and negative lift coefficient. The use of a rear spoiler can effectively increase negative lift without adding too much weight. This can help improve the car's grip and ensure a stable ride on a complex track. However, negative lift is often accompanied by resistance generation, so it is necessary to coordinate the two aerodynamic characteristics of negative lift and resistance to make the rear spoiler perform at its best.

At present, some researchers have carried out research on the rear spoiler of racing cars. He Yibin et al [1]. have carried out research on the influence of the pneumatic rear spoiler on the handling stability of vehicles, designed various control schemes considering relevant performance indices, and verified the schemes through numerical simulation or experimental methods. Mao Xu et al [2]. adopted the numerical simulation method to carry out aerodynamic analysis and comparison of structural parameters such as the airfoil, attack angle, and ground clearance of the rear spoiler of an F1 racing car, studied the drag force and negative lift characteristics of the rear spoiler, and found that the airfoil with a larger curvature and a thicker airfoil body was the optimal solution. Based on the Reynolds mean turbulence equation and Realizable $k-\varepsilon$ turbulence model, Bai Qiuyang et al [3]. established a three-dimensional simulation model of the outflow field of racing cars. Using the orthogonal experimental design method, they analyzed the degree of influence of different racing car kit combinations on racing cars and found that the constant airfoil is the most important for the aerodynamic characteristics of racing cars. Wenhua L et al [4]. studied the spoiler at different positions, and through CFD numerical analysis, they finally found that only the fixed-wind airfoil at high velocity has positive effects, and otherwise it will have more negative effects. Kurec et al [5]. analyzed a scheme for rapidly changing aerodynamic loads on the body and airfoils using two movable spoilers, which required less energy and responded very quickly.

With the development of computer simulation technology, the computational fluid dynamics (CFD) method, which uses computers to solve the flow field in the field of racing cars, is being applied more and more. This paper will use several classic airfoils as its main research object. Firstly, three-dimensional modeling of airfoils is carried out by NX UG software, and then numerical simulation is carried out by Ansys Fluent software. The influence of velocity, attack angle, and airfoils on negative lift and resistance is studied emphatically. The results provide data support for the further optimization of the rear spoiler of racing cars.

2. Methodology

2.1. Geometric model

We adopted the straight RAE2822 airfoil, whose airfoil section is shown in Figure 1.

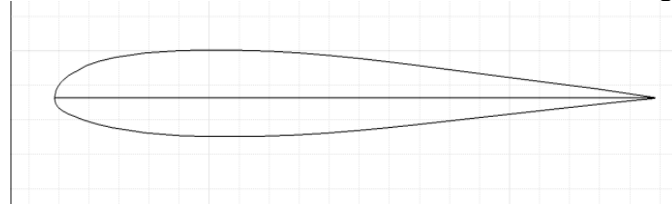


Figure 1. The section line of the RAE2822 airfoil.

We imported the airfoil into 3D modeling software to generate the airfoil. The wingspan length of the generated airfoil is 700 mm and the relative thickness is 20 mm. The generated airfoil shape is shown in Figure 2.

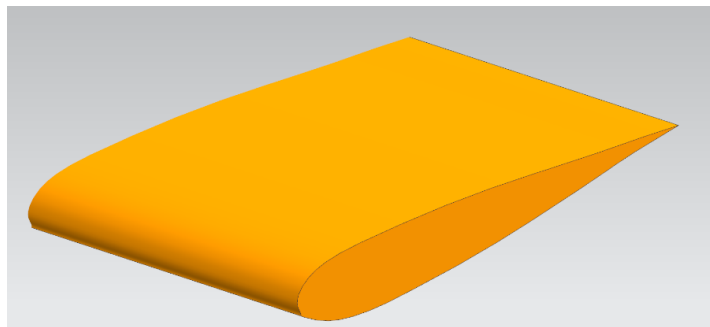


Figure 2. The straight airfoil model.

Several other airfoils include the NACA0015 airfoil, the NASA SC (2)-0410 airfoil, and the NASA SC (2)-0712 airfoil, as shown in Figures 3-5.

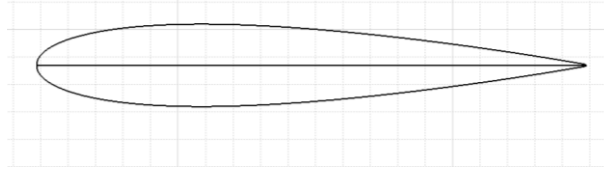


Figure 3. The section line of the NACA0015 airfoil.

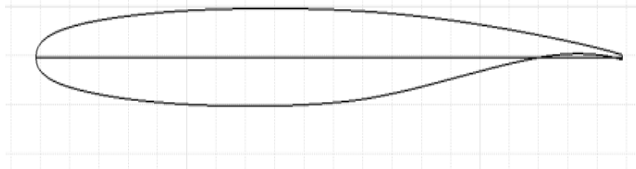


Figure 4. The section line of the NASA SC (2)-0410 airfoil.

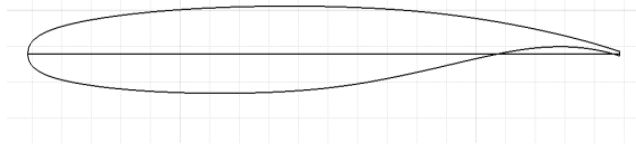


Figure 5. The section line of the NASA SC (2)-0712 airfoil.

Due to the particularity of hydrodynamics research, the actual research object is not the airfoil itself but the flow field around it. Therefore, it is necessary to construct an area around the airfoil and carry out the difference calculation with the airfoil to get the flow field area around the airfoil. This part is called the computational geometry area. The selection of the computational geometry area is strictly restricted; if the area is too large, a large number of grids will be needed in the calculation, and the calculation time will be greatly extended. If the area is too small, information such as the boundary layer around the airfoil may not be fully reflected, thus making the simulation results unreliable. It is generally believed that the dividing standard of the computational geometric area is as follows: the height of the lower and lower fields on the airfoil should be 3 times the average thickness of the airfoil; the width of the left and right flow fields should be twice the wingspan length; the length of the chord length of the airfoil should be 1.5-2 times the length of the front of the airfoil; and the length of the rear should be 2.5-3 times. The calculated geometric area established according to this principle is a cuboid with length * width * height = 2100mm * 2100mm * 360mm, as shown in Figure 6.

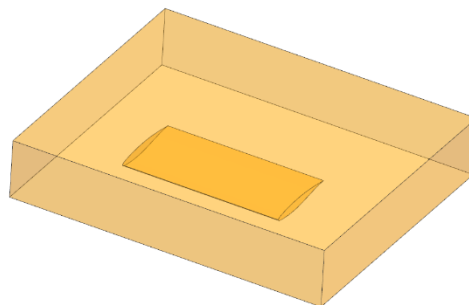


Figure 6. Computational geometry cross-section diagram.

2.2. Fundamental theory

The fluid motion follows the Navier-Stokes equations:
momentum equation:

$$\frac{D\vec{V}}{Dt} = \vec{f}\vec{b} - \frac{1}{\rho}\nabla p + \frac{\mu}{\rho}\nabla^2\vec{V} + \frac{1}{3}\frac{\mu}{\rho}\nabla(\nabla \times \vec{V}) \quad (1)$$

energy equation:

$$\rho \frac{D}{Dt} \left(\hat{u} + \frac{V^2}{2} \right) = \rho \vec{f}\vec{b} \times \vec{V} + \nabla(\vec{V} \times \tau_{ij}) + \nabla(\lambda \nabla T) + \rho \dot{q} \quad (2)$$

continuity equation:

$$\frac{\partial \rho}{\partial t} + \nabla \times (\rho \vec{V}) = 0 \quad (3)$$

Among them: $\frac{D\vec{V}}{Dt}$ term represents the change in the momentum of the fluid over time, or what is called the inertial force term.

$\vec{f}\vec{b}$ is called the body force term.

$-\frac{1}{\rho}\nabla p$ is called the pressure difference term

$\frac{\mu}{\rho}\nabla^2\vec{V} + \frac{1}{3}\frac{\mu}{\rho}\nabla(\nabla \times \vec{V})$ is called the viscous force term

$\frac{\partial \rho}{\partial t}$ term represents the increase in mass at some point in space

$\nabla \times (\rho \vec{V})$ term represents the mass coming out of that point

$\rho \frac{D}{Dt} \left(\hat{u} + \frac{V^2}{2} \right)$ term represents the change of total energy (including internal energy and kinetic energy) of fluid micelles.

$\rho \vec{f}\vec{b}$ term represents the work done by volumetric forces on fluid micelles.

$\rho \dot{q}$ term represents the heat received by fluid micelles from the outside world through radiation.

$\nabla(\vec{V} \times \tau_{ij})$ term represents the work done by surface forces (pressure and viscous forces) on fluid micelles.

$\nabla(\lambda \nabla T)$ term represents the heat received by fluid micelles from the outside world through thermal conduction.

At the same time, the lift force and resistance caused by it also follow a certain physical law, which leads to the lift-drag ratio and other formulas:

$$Cl = L/qS \quad (4)$$

$$Cd = \frac{X}{qS} \quad (5)$$

$$\frac{L}{D} = \frac{Cl}{Cd} \quad (6)$$

Among them:

L means lift force

X means resistance

q means dynamic pressure, $q = \rho * \frac{V^2}{2}$

S is the reference area, and usually we choose the airfoil area.

2.3. Boundary conditions

The velocity inlet was adopted, the pressure outlet was set to one atmosphere, and the pressure base solver was used. The air was regarded as an incompressible fluid, and the other walls were regarded as adiabatic non-slip boundaries. The turbulence model was SST k- ω , and the convective term was a second-order upwind scheme with a residual of 1e-3. After the verification of grid-independent solutions, the calculated grid was selected as 2.05 million.

3. Calculation results and comparative analysis

3.1. Flow field analysis

The airfoil RAE2822, with an attack angle of 0° and an inlet velocity of 100 m/s (360 km/h), was selected as the reference working condition. The velocity distribution, flow field pressure distribution, and pressure distribution of the upper and lower airfoils obtained by calculation are shown in Figures 7-10.

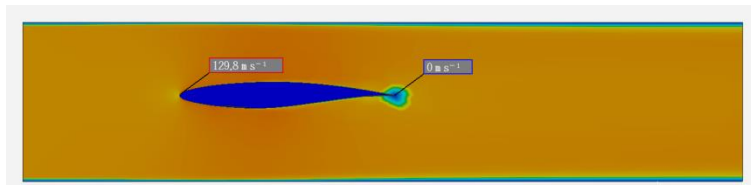


Figure 7. Velocity distribution.

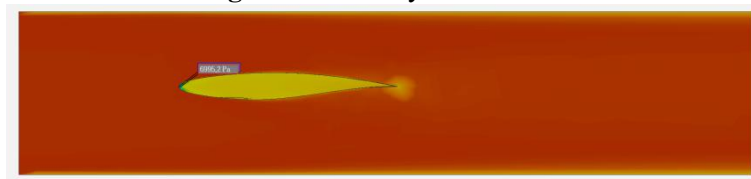


Figure 8. Pressure distribution in the flow field.

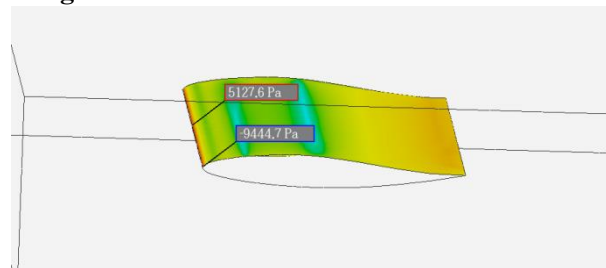


Figure 9. Upper airfoil pressure distribution.

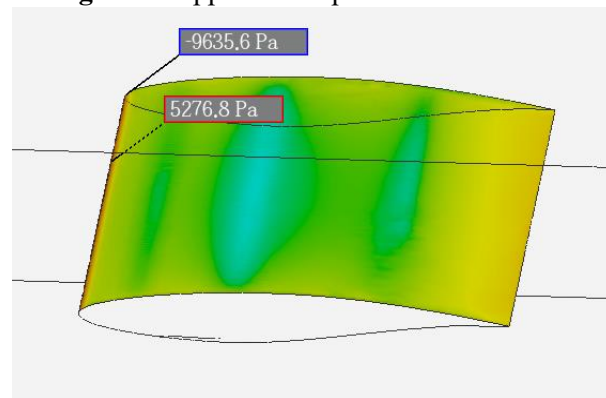


Figure 10. Lower airfoil pressure distribution.

3.2. Influence of attack angle on aerodynamic performance of rear spoilers

Under the base working condition, we adjusted the attack angle to 10° , 20° , 30° , and 40° , respectively, and analyzed the drag force and negative lift generated by the tail and their ratio, namely the lift-drag ratio, as shown in Figure 11.

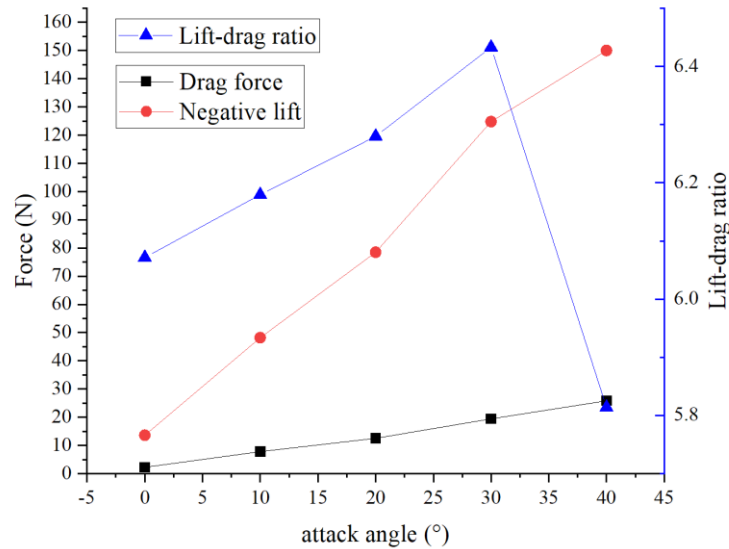


Figure 11. Influence of attack angle on aerodynamic performance.

We can see that with the attack angle increasing, the drag force and negative lift will both increase. However, before 30°, the negative lift tends to rise rapidly, and at 40°, the lift-drag ratio has begun to decline, which means that the drag force gain will be small if the attack angle continues to increase at this time.

3.3. Influence of velocity on the aerodynamic performance of the rear spoiler

Under the base working condition, we adjusted the velocity to 40 m/s, 60 m/s, 80 m/s, and 120 m/s. The negative lift and resistance are shown in Figure 12.

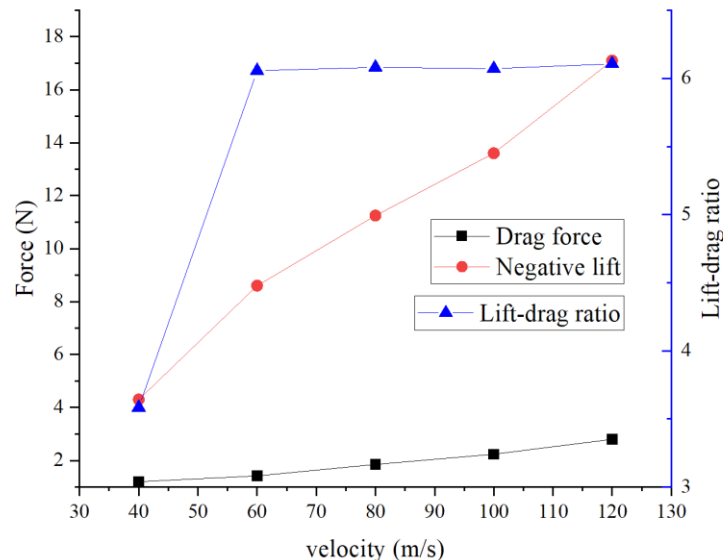


Figure 12. Influence of velocity on aerodynamic performance.

We can see that the drag force is almost directly proportional to the velocity, while the negative lift increases rapidly as the velocity increases. This means that when the car is slow, the drag force provided by the rear spoiler is little or negligible. The lift-drag ratio increases obviously with the increase of velocity, and then maintains at a fixed level.

3.4. Influence of airfoils on the aerodynamic performance of the rear spoiler

We have calculated and compared the RAE2822 airfoil, the NACA0015 airfoil, the NASA SC (2)-0410 airfoil, and the NASA SC (2)-0712 airfoil respectively. The aerodynamic performance of each airfoil under the reference condition is shown in Figure 13.

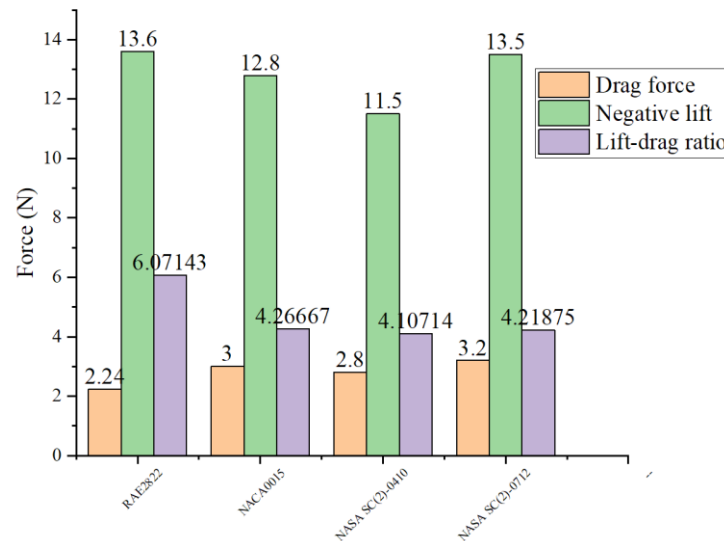


Figure 13. Influence of airfoils on the aerodynamic performance

As can be seen from the figure above, the performances of the four airfoils are quite different, especially the last three. This is because the latter three airfoils belong to supercritical spoilers, which can only show good aerodynamic performance when the velocity is close to the velocity of sound. The velocity of the racing car is generally difficult to exceed 1/3 mA, which is still in the low velocity category.

4. Conclusion

Through the above research, the following conclusions can be drawn within the parameter range of this paper:

1. The maximum lift-drag ratio can be obtained when the attack angle of the rear spoiler is around 30°.
2. The negative lift and the drag force of the rear spoiler are positively correlated with the velocity, and the relationship is basically linear when the velocity exceeds 60 m/s.
3. In this paper, we study the four airfoil types carefully. The RAE2822 airfoil's performance is relatively good and can be acquired at low velocity with a high lift-drag ratio.

References

- [1] He Yibin, Li Weiping, Liu Mengxiang, et al. Aerodynamic characteristics of the rear spoiler of a Formula 1 racing car [J]. Journal of Aerospace Power, 2013(10):5.
- [2] Mao Xu, Wu Ningning. Improved aerodynamic performance of FSAE's new rear spoiler [J]. Mechanical Science and Technology, 2014, 33(09):1397-1402. DOI: 10.13433/j.cnki.1003-8728.2014.0924
- [3] Lei Gengqi, Huang Zhifu, Huang Huazhi. Design of aerodynamics kit for formula student racing car [J]. Auto Motor und Sport, 2020(2):5.
- [4] Wenhua, L. I., and G. Sun. "Car rear spoiler CFD analysis of auxiliary brake performance." Journal of Liaoning Technical University (Natural Science) (2016).
- [5] Krzysztof Kurec, Michał Remer, Tobiasz Mayer, et al. Flow control for a car-mounted rear wing, International Journal of Mechanical Sciences, Volume 152, 2019, Pages 384-399, <https://doi.org/10.1016/j.ijmecsci.2018.12.034>.